Full Length Article

Aberrantly elevated Wnt signaling is responsible for cementum overgrowth and dental ankylosis

Yan Wu[a,b,1], Xue Yuan[b,1], Kristy C. Perez[b], Sydnee Hyman[b], Liao Wang[b,c], Gretel Pellegrini[d], Benjamin Salmon[e], Teresita Bellido[d], Jill A. Helms[b,*]

[a] Orthodontic Department, Stomatology Hospital of Chongqing Medical University, Chongqing Key Laboratory of Oral Disease and Biomedical Sciences, Chongqing Municipal Key Laboratory, Chongqing 401147, China
[b] Division of Plastic and Reconstructive Surgery, Department of Surgery, Stanford School of Medicine, Stanford, CA 94305, USA
[c] State Key Laboratory of Oral Diseases, West China Hospital of Stomatology, Sichuan University, Chengdu 610041, China
[d] Department of Anatomy and Cell Biology, Department of Medicine, Division of Endocrinology, Indiana University School of Medicine and Roudebush Veterans Administration Medical Center, Indianapolis, IN 46022, USA
[e] Paris Descartes University - Sorbonne Paris Cité, EA 2496 - Orofacial Pathologies, Imaging and Biotherapies Lab and Dental Medicine Department, Bretonneau Hospital, HUPNVS, AP-HP, Paris, France

ARTICLE INFO

ABSTRACT

Vertebrate teeth are attached to the jawbones using a variety of methods but in mammals, a fibrous connection is the norm. This fibrous periodontal ligament (PDL) allows teeth to move in the jawbones in response to natural eruptive forces, mastication, and orthodontic tooth movement. In some disease states the PDL either calcifies or is replaced by a mineralized tissue and the result is ankylosis, where the tooth is fused to the alveolar bone. To understand how the PDL maintains this fibrous state, we examined a strain of mice in which tooth movement is arrested. Daβcat[Ot] mice express a stabilized form of β-catenin in DMP1-positive alveolar bone osteocytes and cementocytes, which results in elevated Wnt signaling throughout the periodontium. As a consequence, there is an accrual of massive amounts of cellular cementum and alveolar bone, the PDL itself calcifies and teeth become ankylosed. These data suggest that to maintain its fibrous nature, Wnt signaling must normally be repressed in the PDL space.

1. Introduction

The periodontium is a tripartite structure consisting of a connective tissue, the periodontal ligament (PDL) and two mineralized tissues, the cementum and alveolar bone. The PDL spans the two mineralized tissues and this arrangement permits movement of the teeth within the jawbones. For example, in response to mastication the PDL dissipates potentially damaging strains that would otherwise accumulate in the bone and tooth [1]. Fibrous tissues that serve this type of function are referred to as entheses [2,3]. In health, entheses remain fibrous in nature even though they express osteogenic proteins [4]. In some disease states, entheses mineralize and this results in a condition known as ankylosis, where a joint becomes immobile.

Biological signals are required to maintain the fibrous state of the PDL (reviewed recently in [5]). For example, the transcription factor Scleraxis actively prevents mineralization, in part by opposing the effects of the transcription factor Osterix [6]. Physical signals - both tensile and compressive - are also implicated in maintaining the fibrous nature of the PDL [3]. Whether biological signals, physical stimuli, or a combination of both are required to maintain the fibrous state of the PDL, one thing is certain: if the PDL has inappropriately undergone mineralization then teeth become immobile [7–10]. Dental ankylosis represents a pathologic condition in mammals but in stem mammals including extinct flying and aquatic reptiles and dinosaurs, dental ankylosis was the natural terminal stage in successful tooth replacement [11].

To gain insights into the mechanisms regulating the development and potentially, evolution of the periodontium, we undertook an analysis of a strain of mice in which tooth movement is defective. Daβcat[Ot] mice express a stabilized form of β-catenin in osteocytes [12], and exhibit defects in the movement of both incisors and molars. We combined molecular, cellular, histologic, and imaging analyses to understand how a stabilized form of β-catenin led to prolonged Wnt/β-catenin signaling in alveolar bone osteocytes and surprisingly, in

cementocytes as well, and how this aberrant Wnt signal led to dental ankylosis through mineralization of the PDL.

2. Methods and materials

2.1. Animals

The generation of daβcat^{Ot} mice was approved by the Institutional Animal Care and Use Committee of Indiana University School of Medicine. Every effort was taken to ensure the guiding principles of the three R's (Replacement, Reduction, and Refinement) were followed (Animal research: Reporting of in vivo experiments 2016). All mice were housed in a temperature-controlled environment with 12 h light/dark cycles. Daβcat^{Ot} mice were generated by crossing dentin matrix acidic phosphoprotein 1(DMP1)-8kb-Cre mice with Catnb^{lox(ex3)} mice, in which exon 3 that encodes for β-catenin degradation is flanked by LoxP sites [12]. Hemizygous DMP1-8kb-Cre^{+/−} mice were crossed with homozygous Catnb^{lox(ex3)/lox(ex3)} mice. The cross rendered 50% DMP1-8 kb-Cre^{+/−}; Catnb^{lox(ex3)/+} (daβcat^{Ot} mutant mice) and 50% controls Catnb^{lox(ex3)/+} mice (daβcat^{Ot} control mice). The skeletal phenotype of the DMP1-8kb-Cre^{+/−} and Catnb^{lox(ex3)/+} mice is indistinguishable from the wild-type C57BL/6 mice. Mice expressing green fluorescent protein (GFP) in osteocytes (DMP1^{GFP}) [13,14] were bred with Catnb^{lox(ex3)/lox(ex3)} or daβcat^{Ot} mice to identify the cells expressing DMP1.

2.2. Micro-computed tomography analysis

Micro-computed tomography (μCT) scans of murine skulls were performed on daβcat^{Ot} control ($N = 3$) and daβcat^{Ot} mutant ($N = 3$) groups. Mice were sacrificed, tissues were fixed in 70% ethanol and then scanned at 10 μm resolution (Micro XCT, Xradia Inc., Pleasanton, CA). Samples were reconstructed, segmented with ScanIP then using the measure function, the length of incisors were calculated. After orienting the μCT slice planes to show longitudinal sections of the incisors, the length of root-to-tip was measurements and the average length of 3 mice were calculated.

2.3. Histology, immunohistochemistry, and histomorphometric analyses

Animals were sacrificed at the time points indicated by first anesthetizing them with an IP injection of ketamine (80 mg/kg) and Xylazine (16 mg/kg) followed by cervical dislocation. Tissues were fixed in 4% paraformaldehyde overnight then washed in PBS for 30 min and decalcified in 19% EDTA for up to 14 days in 4 °C, with shaking. After decalcification, specimens were dehydrated through an ascending ethanol series and embedded in paraffin. Eight-micron-thick longitudinal, transverse, and coronal sections were cut and collected on superfrost-plus slides. Movat's pentachrome staining was performed on slides [15], further dehydrated in an ethanol series, and then mounted with Permount. Tartrate resistant acid phosphatase (TRAP) staining was performed [16]. Immunohistochemistry was performed [17] with primary antibodies: rabbit anti-PCNA (ab18197, Abcam, Cambridge, UK), rabbit anti-Periostin (ab14041, Abcam), rabbit anti-Osterix (ab22552, Abcam), mouse anti-Sclerostin (AF1589, R&D systems, Minneapolis, USA), mouse anti-CTNNB1 (β-catenin) antibody (610154, BD Biosciences New Jersey, USA), rabbit anti-green fluorescent protein (GFP; 2956S, Cell Signaling Technology, Danvers, USA) and secondary antibodies including biotinylated goat anti-rabbit IgG antibody (BA-1000, Vector Lab, Burlingame, USA) and biotinylated horse anti-mouse IgG antibody (BA-2000, Vector Lab). The staining was visualized by ABC peroxidase standard staining kit (32020, Thermo Fisher Scientific, Rockford, USA). Tissue sections were photographed using a Leica digital imaging system.

Histomorphometry was performed using Image J software (Version 1.49v) to quantify the TRAP activity. At least 4 slides from each sample were used for quantification. The total length of incisor was divided into three parts from the tip to the apex. The first 1/3 part was defined as the region of interest (ROI) for the incisive edge and the third 1/3 was used for apex quantification. To quantify the cell number in PDL area, the total DAPI^{+ve} cell in PDL area are counted and normalized to the PDL area.

2.4. Statistical analyses

Results were presented as mean ± standard deviation. A two-tailed Student's t-test was used to determine significant differences between data sets. A p value < 0.05 was considered statistically significant and all statistical analyses were performed with Microsoft Excel software (Version 15.16, USA).

This study follows ARRIVE guidelines.

3. Results

3.1. Tooth eruption is perturbed in daβcat^{Ot} mice

A functional periodontium is required for active tooth eruption [18,19], and in murine incisors this eruption process continues throughout life. In daβcat^{Ot} mice, however, incisor eruption was arrested. Compared with μCT scans of P42 littermate controls (Fig. 1A,C), the mandibular incisors of aged-matched daβcat^{Ot} mutant mice were not visible in the oral cavity (Fig. 1B,D). In control littermates, the incisor tip (green asterisk) projected past the most coronal extent of the alveolar ridge (white arrow; Fig. 1E) whereas in daβcat^{Ot} mice the incisor tip (red asterisk) was still encased in alveolar bone (white arrow; Fig. 1F; quantified in G). Upon close examination, the PDL near the incisor tip was thin and discontinuous with no obvious fibrous attachment between the bone and the lingual incisor surface (Fig. 1F).

One explanation for this phenotype could be a lack of adequate tooth structure; in other words, the eruption machinery was intact but there was insufficient tooth material to protrude into the oral cavity. The overall lengths of the maxillary incisors in controls and mutants, however was equivalent (Fig. 1H,I), yet one erupts and the other doesn't fully erupt (Fig. 1A–D). Therefore, it was unlikely the case that the eruption defect in daβcat^{Ot} mice was solely caused by inadequate tooth structure.

Three-dimensional volumetric reconstruction data revealed that overall, the mandibular daβcat^{Ot} incisors were significantly shorter than controls (Fig. 1J,K). We considered cellular mechanisms of incisor eruption in rodents. For example, cell proliferation at the rodent incisor apex drives eruption [20–22]. Using PCNA immunostaining, we identified proliferating cells in controls (Fig. 1L) and the number of PCNA^{+ve} cells was notably reduced in the mutants (Fig. 1M). We also noted a defect in molar eruption (Fig. 1A,B) but PCNA staining failed to reveal any proliferating cells at the apices of these teeth (data were not shown). Therefore, it was unlikely that a lack of cell proliferation was solely responsible for the widespread eruption defect and turned to consider other mechanisms that could contribute to this phenotype.

3.2. The daβcat^{Ot} eruption defect is not due to perturbed osteoclast activity

Osteopetrosis is a genetic condition of increased bone mass caused by defects in osteoclast formation and function [23]. Osteopetrosis can arrest tooth movement [24] because the alveolar bone fails to resorb properly [25,26]. To ascertain whether the daβcat^{Ot} eruption defect was attributable to an osteopetrotic phenotype we evaluated osteoblast and osteoclast function around the roots using ALP and TRAP activities (Fig. 2A,B). In controls, ALP and TRAP activities was readily detectable in the alveolar bone surrounding the molar roots (Fig. 2A), as well as around the incisor buccal and lingual alveolar bone surfaces (Fig. 2C,D). In daβcat^{Ot} mutants, TRAP activity was evident around the alveolar bone surrounding the molar roots (Fig. 2B) and along the
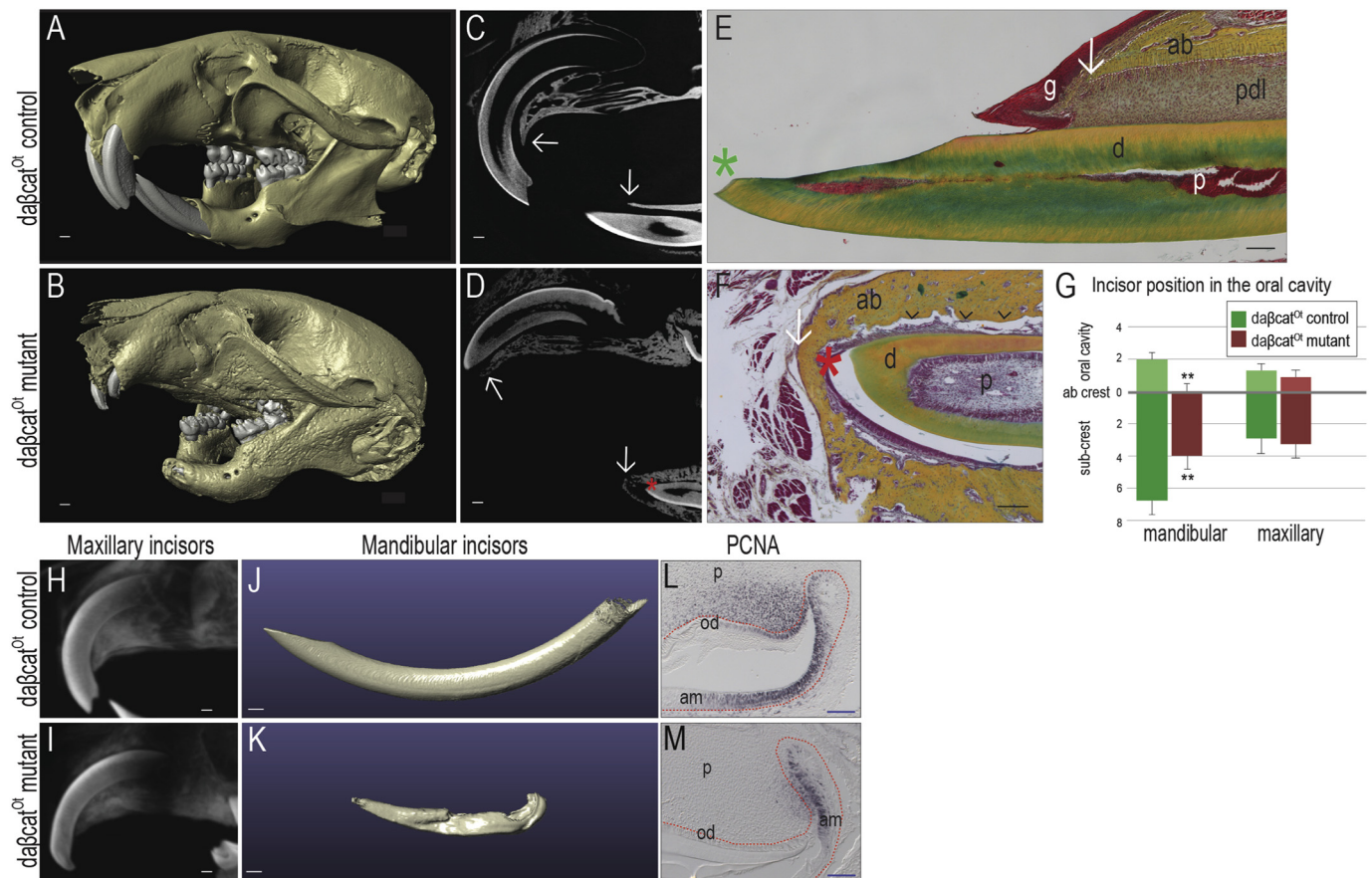
Fig. 1. Tooth eruption is perturbed in daβcat^{Ot} mice.

Micro-computed tomographic scans of the skull showed (A) normal incisor and molar tooth positions in P42 daβcat^{Ot} control mice; (B) in contrast, daβcat^{Ot} mutant littermates had shortened upper incisors and no visible mandibular incisors, and no visible maxillary first molars. In addition, the alveolar bone of daβcat^{Ot} mutant mice appeared mottled in comparison to control littermates. (C) Sagittal μCT sections show the fully formed, erupting incisors of daβcat^{Ot} control mice; arrows indicate the position of the crest of the alveolar bone relative to the maxillary and mandibular incisors. (D) In daβcat^{Ot} mutant littermates, μCT sections show the presence of incisor tooth structure (red asterisk) that has not erupted past the alveolar bone crest (white arrows). (E) Representative sagittal tissue sections stained with pentachrome illustrate that in P42 daβcat^{Ot} controls, the incisor tip (green asterisk) projects past the most crestal extent of the alveolar bone (white arrow). PDL fibers are evident on the lingual surface of the incisor whereas (F) in daβcat^{Ot} mutants, there is no corresponding PDL (black arrowheads). In addition, the incisor tip (red asterisk) remains encased in alveolar bone (white arrow). (G) Quantification of the relative position measured in mm, of mandibular and maxillary incisors in daβcat^{Ot} control and mutant mice ($N = 3$). (H,I) μCT sections of maxillary incisors in P42 (H) daβcat^{Ot} controls and (I) daβcat^{Ot} mutants. (J,K) Volume rendering of μCT data demonstrate (J) normal morphology of the mandibular incisors compared to (K) the truncated morphology of P42 daβcat^{Ot} mutant incisors. (L,M) PCNA staining identifies proliferating cells in the cervical loop of (L) control and (M) daβcat^{Ot} mutants at P24. **$p < 0.01$. Abbreviations: ab, alveolar bone; d, dentin; g, gingiva; p, pulp; pdl, periodontal ligament; od, odontoblasts; am, ameoblasts. Scale bars: white = 500 μm; black = 100 μm; blue = 50 μm. (For interpretation of the references to color in this figure legend, the reader is referred to the web version of this article.)

thickened buccal and lingual alveolar bone surfaces (Fig. 2E,F). The extent of TRAP staining was quantified, and these analyses showed that rather than being depressed, daβcat^{Ot} mutants had significantly higher osteoclast activity compared to controls (Fig. 2G). These data agree with previously published analyses of the daβcat^{Ot} strain [12]. Notably, in some regions, the low density PDL space is missing and the alveolar bone appears to be fused with the tooth (Fig. 2E, yellow boxes).

3.3. Daβcat^{Ot} mutants lack a function periodontal ligament

The daβcat^{Ot} eruption defect was not due to an arrest in bone resorption nor was it due to a primary defect in osteoclast activity; we therefore considered other explanations for the tooth eruption defect in daβcat^{Ot} mutants. For example, tooth movement is possible because of the fibrous nature of the PDL (Fig. 3A); we reasoned that changes in the width and/or its fibrous state might adversely affect tooth eruption. We first determined there was a narrowing of the PDL space in the mutant: at post-natal day 24 (P24), histomorphometric comparisons between the strains revealed a slightly reduced PDL space in daβcat^{Ot} mutants

(compare Fig. 3A,B; quantified in E). Histomorphometric comparisons were made again at P42. The PDL normally widens until animals reach adulthood, which was seen in the control group (compare Fig. 3A,C). In daβcat^{Ot} mutants, however, the PDL instead had narrowed significantly (Fig. 3D, quantified in E). Closer analyses revealed aberrant mineralization within the PDL proper that appeared like "spot-welds" (arrows) within what is a normally fibrous tissue (compare Fig. 3F,G). These observations together suggested that the mineralized tissues surrounding the PDL e.g., the alveolar bone and/or cementum were either enroaching onto the PDL space, or that the PDL itself was undergoing mineralization. μCT imaging analyses verified the widespread nature of this aberrant mineralization: normally, the PDL appears as a dark "halo" around teeth (Fig. 3H) but in daβcat^{Ot} mutants, the radiolucent area was replaced in places by a radio-opaque tissue (arrows, Fig. 3I).

To further examine the fibrous versus mineralized state of the daβcat^{Ot} PDL, we examined daβcat^{Ot} control and mutant mice for the expression of Periostin. Periostin is normally expressed in the fibrous PDL (Fig. 3J) but was minimally detectable in the daβcat^{Ot} mutant
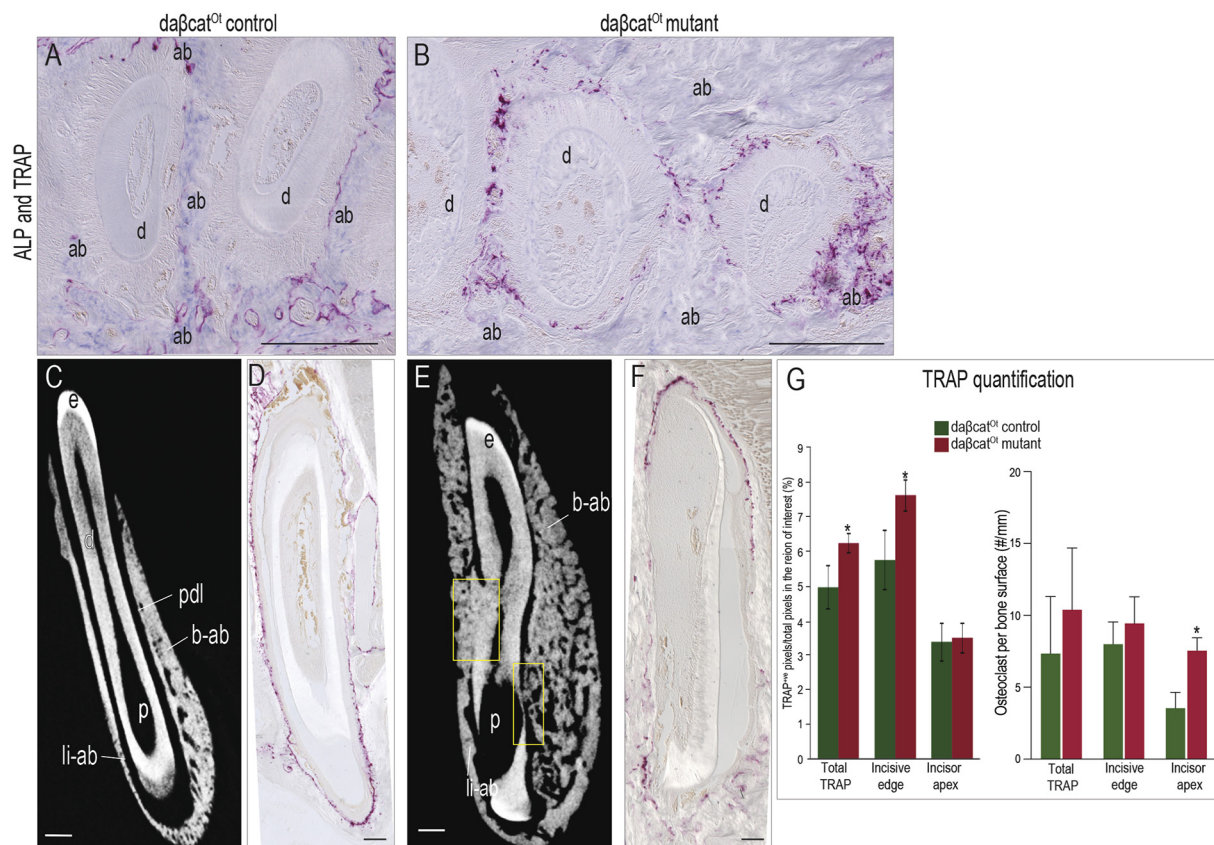
Fig. 2. The arrest in tooth eruption is not attributable to defective osteoclast activity in daβcat^Ot mice.
TRAP and ALP double staining showing bone resorption and bone formation in P42 (A) daβcat^Ot control mice and (B) daβcat^Ot mutant mice. (C) Representative sagittal μCT sections in P42 control daβcat^Ot incisors, showing the relative thickness of the buccal and lingual alveolar bone plates and the low density PDL space. (D) TRAP activity along the buccal alveolar bone surface near the incisive edge and along the lingual alveolar bone surface near the apex. (E) Representative sagittal μCT sections in P42 mutant daβcat^Ot incisors, showing the significantly thicker buccal alveolar bone plate. In some regions, the low density PDL space is missing and the alveolar bone appears to be fused with the tooth (yellow boxes). (F) TRAP activity is detectable along the buccal and lingual alveolar bone plates. (G) Quantification of TRAP activity around the erupting incisors of daβcat^Ot control and mutant mice ($N = 6$). Abbreviations: as indicated previously and e, enamel; b-ab, buccal alveolar bone plate; li-ab, lingual alveolar bone plate. Scale bars = 500 μm. (For interpretation of the references to color in this figure legend, the reader is referred to the web version of this article.)

(Fig. 3K). On tissue sections from daβcat^Ot mutants, we found that in sites that still retained a fibrous PDL, the osteogenic protein Osterix was expressed very strongly (compare Fig. 3L,M). Did this change in Osterix result from a direct increase in the number of osteogenic cells in the daβcat^Ot mutant PDL? To address this question, we verified that cell proliferation in the daβcat^Ot mutant PDL, just like in an adult wild-type PDL [4], was minimal (data were not shown). We then performed DAPI staining to quantify the density of cells in the PDL area in both daβcat^Ot control and mutant mice. The number of DAPI^+ve cells in PDL was normalized to the area. These data demonstrated that although the PDL space was narrower in the daβcat^Ot mutant group, cell density was comparable to the control group (Fig. 3N,O, quantified in P). Finally, to confirm that the Osterix^+ve cells were indeed committed to an osteogenic fate, expression of a late-stage osteogenesis marker [27,28], Osteocalcin, was examined. Osteocalcin is normally absent from PDL cells (Fig. 3Q) but Osteocalcin^+ve cells were present in the PDL of daβcat^Ot mutant (Fig. 3R). Together, these data demonstrated that the increase in osteogenic cells within the PDL of daβcat^Ot mutant was directly due to a greater percentage of PDL cells committing to an osteogenic fate.

3.4. Sustained Wnt/β-catenin signaling in the periodontium causes ankylosis

Thus far our data demonstrated that the replacement of a fibrous PDL by mineralized tissue was the primary cause of ankylosis in daβcat^Ot mutants. Our next analyses set out to determine how amplified Wnt signaling in the daβcat^Ot mice specifically caused dental ankylosis.

In the appendicular skeleton of daβcat^Ot mutants, sustained Wnt/β-catenin signaling in osteocytes causes a high bone mass phenotype [12]. Osteocyte expression of a stabilized form of β-catenin was achieved using a DMP1 Cre reporter strain [14]. To identify cell populations expressing the stabilized form of β-catenin, we examined DMP1^GFP/daβcat^Ot mice for GFP expression. Alveolar bone osteocytes (Fig. 4A) were GFP^+ve (Fig. 4B). Likewise, cementocytes (Fig. 4C) were GFP^+ve (Fig. 4D).

We confirmed that Wnt signaling was elevated in the daβcat^Ot PDL using an antibody to phosphorylated β-catenin. Compared to controls (Fig. 4E), phosphorylated β-catenin expression was higher in daβcat^Ot PDL (Fig. 4F). Sclerostin expression domains were also expanded: normally, Sclerostin is expressed in osteocytes and cementocytes (Fig. 4G) but in daβcat^Ot mutants, its expression was also detected in the PDL (Fig. 4H). We returned to the DMP1 reporter strain of mice, this time focusing on how the daβcat^Ot mutation affected DMP1 expression itself. In comparison to controls, DMP1 expression itself was dramatically increased in daβcat^Ot mutants (Fig. 4I,J, compared with Fig. 4 B,D). Collectively, these data demonstrated that Wnt signaling was aberrantly elevated in the periodontium of daβcat^Ot mice.

We examined the longer-term sequelae of this elevated Wnt signaling in the periodontium. Normally, acellular cementum covers most of the root surface, and cellular cementum is restricted to the root
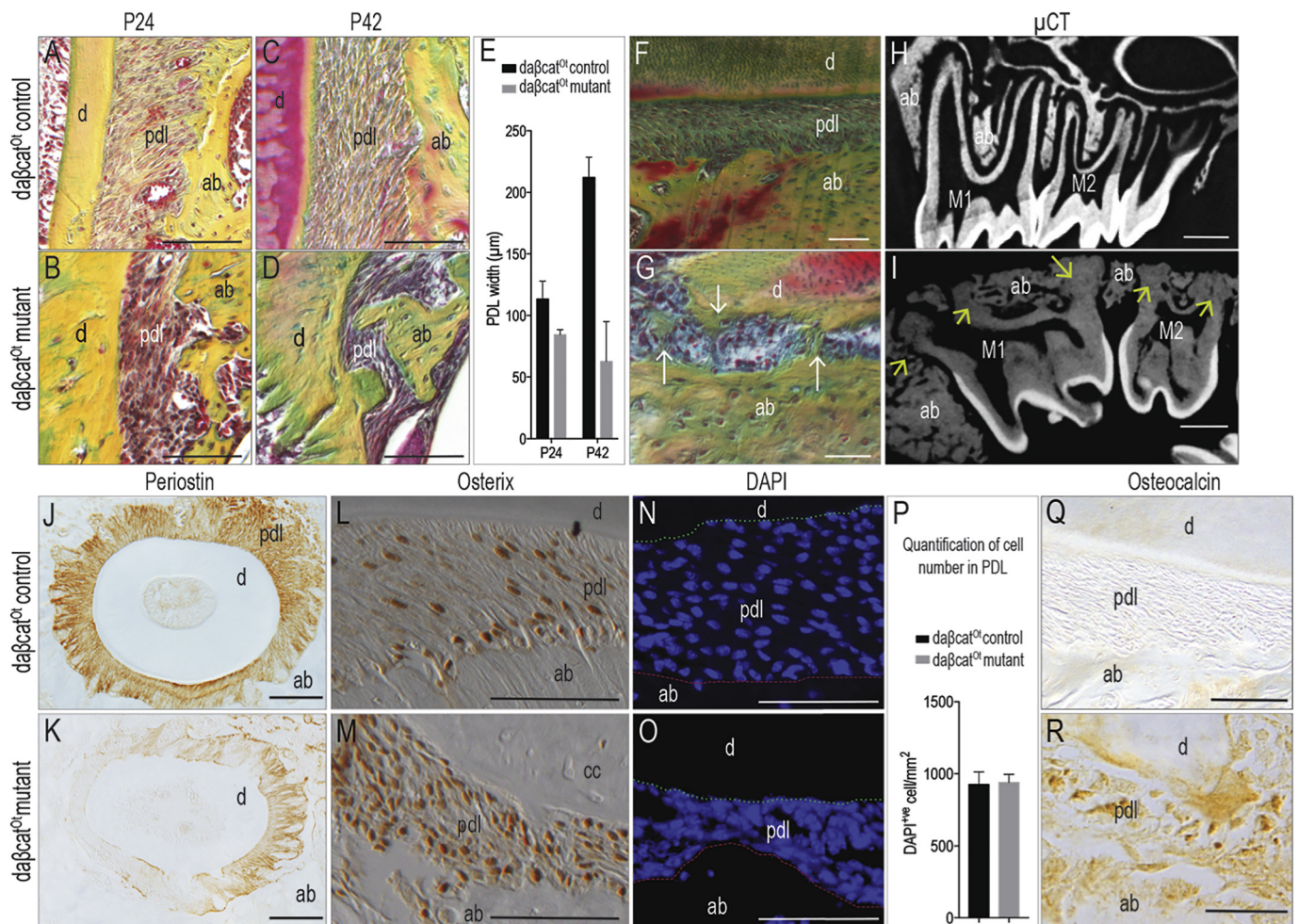
Fig. 3. The fibrous periodontal ligament is obliterated by the daβcat^Ot mutation.

(A,B) Representative pentachrome staining of PDL in P24 (A) daβcat^Ot control mice and their (B) daβcat^Ot mutant littermates. (C,D) Representative pentachrome staining of PDL in P42 (C) daβcat^Ot control mice and their (D) daβcat^Ot mutant littermates. (E) Quantification of PDL width (N = 6). (F) Representative pentachrome staining of P42 molars illustrate the well-aligned fibrous PDL that inserts into alveolar bone and cementum in daβcat^Ot control mice. (G) In daβcat^Ot mutant littermates, the PDL was either replaced by a mineralized tissue (white arrows) or missing altogether. (H) Representative sagittal μCT sections in P42 control daβcat^Ot molars, showing well-developed molar roots and the lucent PDL space surrounding each root. (I) In mutant daβcat^Ot littermates, the roots are truncated and PDL space is largely replaced by a high-density tissue (yellow arrows) that unites the tooth structure and alveolar bone. (J) Periostin is expressed in the PDL of P42 daβcat^Ot control mice that spans from the tooth surface (green dotted line) to the alveolar bone (red dotted line). (K) In daβcat^Ot mutants, Periostin is very weakly expressed in the space between the tooth and alveolar bone. (L) In the PDL of P42 daβcat^Ot control mice, Osterix is expressed most prominently in osteoblasts lining the alveolar bone. Relative to this control, (M) Osterix expression is up regulated in daβcat^Ot mutant mice in the cleft of tissue remaining between the tooth surface and alveolar bone (N = 6). (N) DAPI staining showing the total cell number in the PDL of P42 daβcat^Ot control mice. (O) DAPI staining showing the total cell number in the PDL of P42 daβcat^Ot mutant mice. (P) Quantification of cell number in PDL areas (N = 6). (Q) In the PDL of P42 daβcat^Ot control mice, Osteocalcin is absent. Relative to this control, (R) Osteocalcin expression is observed in daβcat^Ot mutant mice in the cleft of tissue remaining between the tooth surface and alveolar bone (N = 4). Abbreviations: as indicated previously and M1, first molar; M2, second molar; Scale bars: H,I = 1000 μm, others = 100 μm. (For interpretation of the references to color in this figure legend, the reader is referred to the web version of this article.)

apices (Fig. 4K,L). In daβcat^Ot mutants, however, the elevated state of Wnt signaling caused an dramatic expansion in cementum (Fig. 4M,N). At the apex of the root, cellular cementum is normally separated from the adjacent alveolar bone by an intervening fibrous PDL (Fig. 4O). In daβcat^Ot mutants, however, the fibrous PDL was replaced by a solid mass of mineralized tissue (Fig. 4P). This series of events obliterated the distinction between alveolar bone and cellular cementum, and effectively fused the tooth to its socket. Thus, elevated Wnt signaling in multiple components of the periodontium results in the formation of mineralized tissue at the expense of fibrous tissue, thereby resulting in dental ankylosis.

4. Discussion

4.1. Regulating PDL mineralization

Entheses are tissues that must remain fibrous in order to function. In some disease states, as we have shown here, the fibrous PDL enthesis mineralizes and the result is ankylosis. A wide variety of factors - both biological and physical - can influence the mineralization state of entheses. For example, the mineralization state of the cementum can be influenced by a phosphate/pyrophosphate ratio [29] and it is tempting to speculate that a similar general mechanism might underlie mineralization of the PDL. There is no direct data to support this hypothesis, however, and it must be emphasized that, rather than a generalized phenomenon, the aberrant mineralization events in the daβcat^Ot PDL are not uniform. Rather, the mineralization nodes appear more like
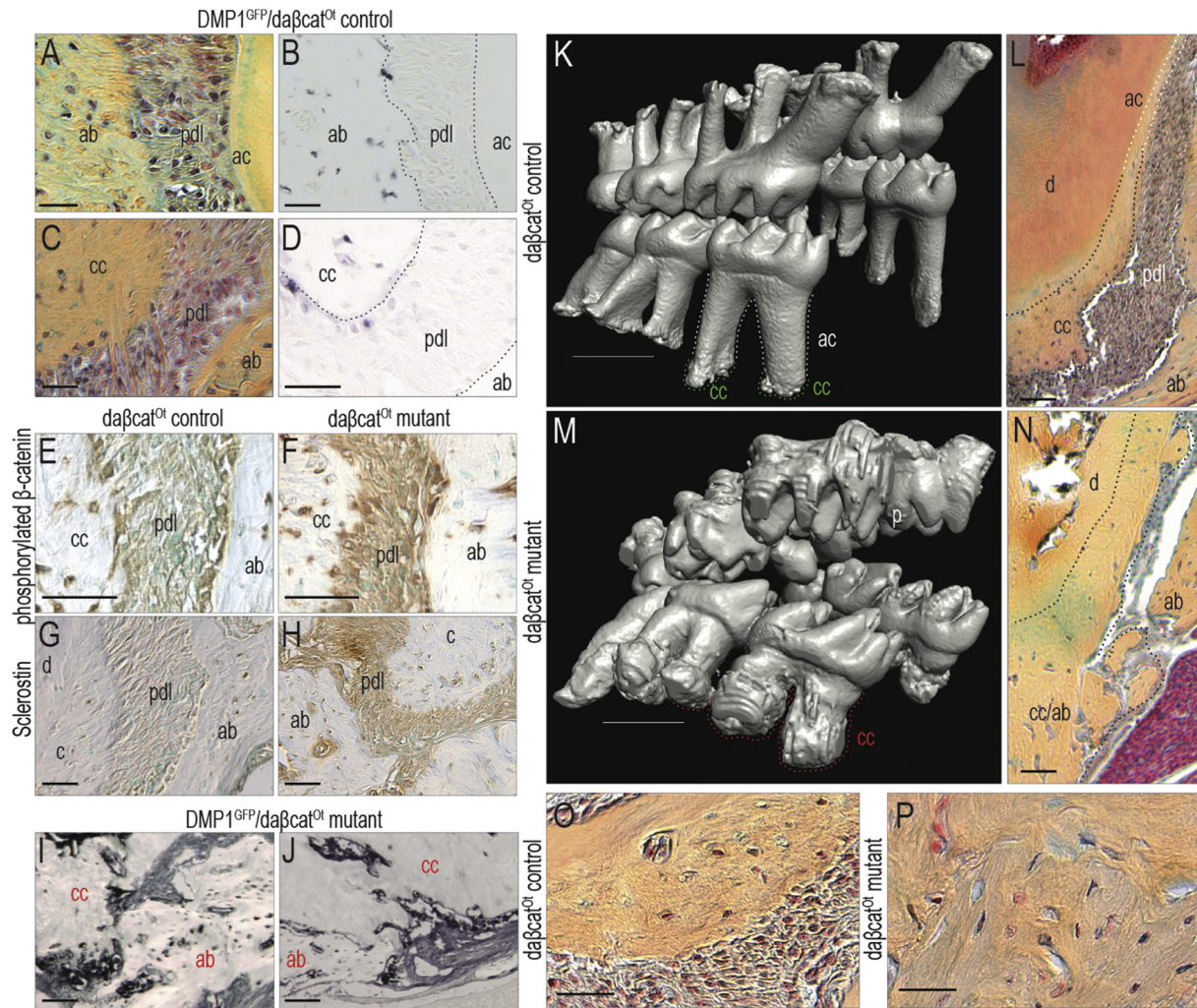
Fig. 4. Sustained Wnt signaling in cells of the cementum and bone produces dental ankylosis.
(A) In the periodontium of P42 DMP1 reporter mice, (B) alveolar bone osteocytes, but not PDL cells, are GFP^{+ve} ($N = 4$). (C) Cementocytes in the cellular cementum of DMP1 reporter mice (D) are also GFP^{+ve}. (E) In control mice (P42), alveolar bone osteocytes, cementocytes, and the PDL cells express a stabilized form of β-catenin. (F) The stabilized form of β-catenin is expressed in broader domains in the daβcat^{Ot} mutant periodontium. (G) In control mice, cementocytes and alveolar bone osteocytes express Sclerostin. (H) Sclerostin expression is notably higher throughout the daβcat^{Ot} mutant periodontium ($N = 6$). (I,J) An expansion in the population of DMP1 expression cells is verified using GFP immunostaining of the P42 DMP1^{GFP};daβcat^{Ot} mutant periodontium ($N = 4$). (K) 3D μCT reconstruction of P42 daβcat^{Ot} control mice showing well-developed molar roots with acellular cementum covering the majority of the root (white dotted line) and cellular cementum restricted at the root apex (green dotted line) ($N = 3$). (L) Pentachrome staining of representative sagittal sections through the P42 daβcat^{Ot} control periodontium, illustrating the boundary between acellular and cellular cementum. (M) daβcat^{Ot} mutant mice have truncated roots encased in cellular cementum (red dotted line). (N) In the daβcat^{Ot} mutant periodontium, root surfaces are covered with cellular cementum. (O) In daβcat^{Ot} controls, cellular cementum at the root apex is juxtaposed to a fibrous PDL. (P) In daβcat^{Ot} mutants, the mineralized tissue of the alveolar bone and cementum are contiguous. Abbreviations: as indicated previously. Scale bars: K,M = 1000 μm, others = 100 μm. (For interpretation of the references to color in this figure legend, the reader is referred to the web version of this article.)

"spot-welds" within a normally fibrous tissue (Figs. 2,3). This complicates a biochemical analysis of the mutant PDL as a tissue, since the mineralization spots are surrounded by fibrous PDL.

Matrix Gla protein (MGP) has also been recognized as a potent calcification inhibitor, which also suggests a potential role in preventing PDL mineralization. In vitro data support this conjecture [30], but again, whether a similar mechanism is at work to maintain a fibrous PDL is simply not known. At least in vitro, the aberrant expression of an extracellular matrix protein such as bone sialoprotein is initially sufficient to promote mineralization, but the effect is transient [31], and so is unlikely to be the causal link in the daβcat^{Ot} ankylosis phenotype.

Another potential clue may come from analysis of ANK, a transmembrane protein that control movement of intracellular inorganic pyrophosphate across the cell membrane [32]. Genetic modulation of ANK in humans and other vertebrates have identified a role in

regulating tissue calcification [32] and potentially, mineral deposition in tendons and ligaments. There is, however, no mention of dental ankylosis in *ank/ank* mice [33]. Clearly, there is still much to be learned about what factors, both biological and physical, are key regulators of mineralization within the functioning PDL.

4.2. Wnt signaling is essential for the homeostasis of the periodontium

An abundance of data demonstrates that Wnt signaling is required for proper development of the periodontium. For example, if Wnt signaling is disrupted early during embryogenesis then eventually the development of the periodontium is arrested [34–36]. If Wnt signaling is disrupted after the periodontium has formed, then homeostasis of the periodontium is disrupted [37,38]. Wnt signaling is also required to maintain alveolar bone [39] and cementum [37]. Given the

interdependence of the cementum, bone, and the PDL on one another during development and homeostasis, it is challenging to unravel just when and where endogenous Wnt signals are having their primary action. Daβcat^{Ot} mutant mice offered rare insights into this conundrum because Wnt signaling was amplified only after the embryonic periodontium had formed [40], and then only in very specific cell niches.

4.3. Elevated Wnt/β-catenin signaling causes mineralization of the PDL

Daβcat^{Ot} mutant mice demonstrate a progressive expansion of Wnt responsive cells that has an unusually detrimental effect on the periodontium. Wnt/β-catenin signaling is normally restricted in alveolar bone osteocytes and cementocytes, but in daβcat^{Ot} mutant mice, Wnt signaling spreads to envelop the entire PDL (Fig. 4). From our analyses of the DMP1 reporter strain, we knew that DMP1 becomes aberrantly expressed in the daβcat^{Ot} mutant PDL (Fig. 4B,D), a conclusion that was validated using DMP1 immunostaining (Fig. 4I,J). Precisely how this expansion in DMP1 expression occurs was not immediately obvious. Our current hypothesis is that the gradual accretion of bone and cementum constricts the PDL space in daβcat^{Ot} mice (Fig. 3A–D). Both osteoblasts and cementoblasts normally produce and respond to Wnt signals (Fig. 4) therefore it is reasonable to speculate that as the PDL space narrows, Wnt signals emanating from the mineralizing tissues begin to impact cells in the middle of the PDL space. The subsequent expression of DMP1 in PDL cells may therefore be a cause - rather than an instigating factor - in PDL mineralization.

While some parts of this hypothesis are still speculative, one thing is clear: as the Wnt responsive cell populations expand so, too, does the mineralized tissues. Within short order, both the volume and distribution of cementum and alveolar bone have enlarged in daβcat^{Ot} mutants (Fig. 4), which together obliterates the fibrous PDL (Fig. 4). Other investigators have shown that stabilizing beta-catenin via an Osteocalcin-Cre reporter strain leads to an accumulation of cellular cementum deposited over the entire molar root surfaces of molar in the mutant mice, which causes a narrowing of the PDL space [41,42]. Likewise, stabilizing beta-catenin via an Col1a1-Cre reporter strain to leads to abnormal tooth eruption and excessive cementum hypoplasia [36]. Neither group, however, reported an eruption defect due to ankylosis, as we have shown here for daβcat^{Ot} mice. Finally, there is the possibility that the ankylosis phenotype in daβcat^{Ot} mice is that because of sustained Wnt signaling, the PDL itself undergoes calcification (Fig. 4). Whether the cementum and bone are simultaneously encroaching on the PDL space, or the PDL itself undergoes mineralization, the end result is a fusion of the cementum to the alveolar bone, which arrests tooth eruption. Collectively, these data also raise a possibility that in order to maintain its fibrous nature, Wnt signaling must normally be repressed in the PDL space. Mechanosensory studies support this relationship between repressed Wnt signaling and a fibrous fate [43,44].

4.4. A pattern of ankylosis

The pattern of ankylosis we observe in the daβcat^{Ot} mutant may reflect the pattern of tooth eruption. For example, the daβcat^{Ot} phenotype is based on conditional expression of a stabilized form of beta-catenin, driven by the DMP1 promoter. Since mandibular molars erupt prior to maxillary molars, we speculate that expression of stabilized beta catenin has not yet reached its maximum in the mandible by the time molars initiate their eruption. Conversely, by the time the maxillary molars erupt the expression of stabilized beta-catenin may have reached its zenith. Analyses of other strains of mice in which Wnt signaling is aberrrantly elevated in the periodontium may shed light on this hypothesis.

4.5. Ankylosis may represent a developmental atavism

In mammals, ankylosis represents a pathological condition that

prevents tooth movement, and our study suggests that its etiology is related to pathologically sustained Wnt signaling. In some animals, however, ankylosis is not a pathologic condition. Rather, it represents a natural stage in odontogenesis [45]. For example, in stem mammals including extinct flying and aquatic reptiles and dinosaurs, dental ankylosis was the norm [46]. In the marine lizard *Mosasauridae*, cellular cementum and alveolar bone accumulated throughout the animal's life, leading to ankylosis [11,47].

This same interpretation aptly describes the daβcat^{Ot} mutant phenotype, where accelerated accumulation of both mineralized tissues eventually causes ankylosis of the molars and incisors. In the case of daβcat^{Ot} mutant mice, the molecular basis for the phenotype is clear; it is tempting to speculate that a similar molecular mechanism of sustained Wnt signaling in the periodontium might have been shared by the *Mosasauridae* tooth attachment apparatus [11].

Disclosure

None of the authors declare a conflict of interest.

Acknowledgements

References

[1] F. Groning, M. Fagan, P. O'Higgins, Modeling the human mandible under masticatory loads: which input variables are important? Anat. Rec. 295 (5) (2012) 853–863.

[2] M. Benjamin, H. Toumi, J.R. Ralphs, G. Bydder, T.M. Best, S. Milz, Where tendons and ligaments meet bone: attachment sites ('entheses') in relation to exercise and/or mechanical load, J. Anat. 208 (4) (2006) 471–490.

[3] S. Thomopoulos, G.M. Genin, L.M. Galatz, The development and morphogenesis of the tendon-to-bone insertion - what development can teach us about healing, J. Musculoskelet. Neuronal Interact. 10 (1) (2010) 35–45.

[4] L. Huang, B. Liu, J.Y. Cha, G. Yuan, M. Kelly, G. Singh, S. Hyman, J.B. Brunski, J. Li, J.A. Helms, Mechanoresponsive properties of the periodontal ligament, J. Dent. Res. 95 (4) (2016) 467–475.

[5] T. de Jong, A.D. Bakker, V. Everts, T.H. Smit, The intricate anatomy of the periodontal ligament and its development: lessons for periodontal regeneration, J. Periodontal Res. 52 (6) (2017) 965–974.

[6] A. Takimoto, M. Kawatsu, Y. Yoshimoto, T. Kawamoto, M. Seiryu, T. Takano-Yamamoto, Y. Hiraki, C. Shukunami, Scleraxis and osterix antagonistically regulate tensile force-responsive remodeling of the periodontal ligament and alveolar bone, Development 142 (4) (2015) 787–796.

[7] D.B. Rodrigues, L.M. Wolford, L.M. Figueiredo, G.Q. Adams, Management of ankylosed maxillary canine with single-tooth osteotomy in conjunction with orthognathic surgery, J. Oral Maxillofac. Surg. 72 (12) (2014) 2419 e1–6.

[8] I. Agabiti, P. Cappare, E.F. Gherlone, C. Mortellaro, G.B. Bruschi, R. Crespi, New surgical technique and distraction osteogenesis for ankylosed dental movement, J. Craniofac. Surg. 25 (3) (2014) 828–830.

[9] K.K. Shi, J.Y. Kim, T.H. Choi, K.J. Lee, Timely relocation of subapically impacted maxillary canines and replacement of an ankylosed mandibular molar are the keys to eruption disturbances in a prepubertal patient, Am. J. Orthod. Dentofac. Orthop. 145 (2) (2014) 229–237.

[10] K.H. You, Y.S. Min, H.S. Baik, Treatment of ankylosed maxillary central incisors by segmental osteotomy with autogenous bone graft, Am. J. Orthod. Dentofac. Orthop. 141 (4) (2012) 495–503.

[11] A.R. LeBlanc, R.R. Reisz, K.S. Brink, F. Abdala, Mineralized periodontia in extinct relatives of mammals shed light on the evolutionary history of mineral homeostasis in periodontal tissue maintenance, J. Clin. Periodontol. 43 (4) (2016) 323–332.

[12] X. Tu, J. Delgado-Calle, K.W. Condon, H. Maycas, H. Zhang, N. Carlesso, M.M. Taketo, D.B. Burr, L.I. Plotkin, T. Bellido, Osteocytes mediate the anabolic actions of canonical Wnt/beta-catenin signaling in bone, Proc. Natl. Acad. Sci. U. S. A. 112 (5) (2015) E478–E486.

[13] A.N. Ben-awadh, J. Delgado-Calle, X. Tu, K. Kuhlenschmidt, M.R. Allen, L.I. Plotkin, T. Bellido, Parathyroid hormone receptor signaling induces bone resorption in the adult skeleton by directly regulating the RANKL gene in osteocytes, Endocrinology 155 (8) (2014) 2797–2809.

[14] I. Kalajzic, A. Braut, D. Guo, X. Jiang, M.S. Kronenberg, M. Mina, M.A. Harris, S.E. Harris, D.W. Rowe, Dentin matrix protein 1 expression during osteoblastic differentiation, generation of an osteocyte GFP-transgene, Bone 35 (1) (2004) 74–82.

[15] H.Z. Movat, Demonstration of all connective tissue elements in a single section; pentachrome stains, A.M.A. Arch. Pathol. 60 (3) (1955) 289–295.

[16] P. Leucht, J.B. Kim, R. Wazen, J.A. Currey, A. Nanci, J.B. Brunski, J.A. Helms, Effect of mechanical stimuli on skeletal regeneration around implants, Bone 40 (4) (2007) 919–930.

[17] S. Minear, P. Leucht, J. Jiang, B. Liu, A. Zeng, C. Fuerer, R. Nusse, J.A. Helms, Wnt proteins promote bone regeneration, Sci. Transl. Med. 2 (29) (2010) 29ra30.

[18] H.N. Newman, Attrition, eruption, and the periodontium, J. Dent. Res. 78 (3) (1999) 730–734.

[19] A.E.W. Miles, C. Grigson, F. Colyer (Eds.), Colyer's Variations and Diseases of the Teeth of Animals, Rev. ed., Cambridge University Press, Cambridge England; New York, 1990.

[20] A.R. Ness, D.E. Smale, The distribution of mitoses and cells in the tissues bounded by the socket wall of the rabbit mandibular incisor, Proc. R. Soc. Lond. B Biol. Sci. 151 (942) (1959) 106–126.

[21] J.R. Gomes, N.F. Omar, E.R. Do Carmo, J.S. Neves, M.A. Soares, E.A. Narvaes, P.D. Novaes, Relationship between cell proliferation and eruption rate in the rat incisor, Anat. Rec. 296 (7) (2013) 1096–1101.

[22] H. Sicher, Tooth eruption: the axial movement of continuously growing teeth, J. Dent. Res. 21 (2) (1942) 201–210.

[23] C. Sobacchi, A. Schulz, F.P. Coxon, A. Villa, M.H. Helfrich, Osteopetrosis: genetics, treatment and new insights into osteoclast function, Nat. Rev. Endocrinol. 9 (9) (2013) 522–536.

[24] M.J. Cielinski, T. Iizuka, S.C. Marks Jr., Dental abnormalities in the osteopetrotic rat mutation microphthalmia blanc, Arch. Oral Biol. 39 (11) (1994) 985–990.

[25] H. Wang, M. Pan, J. Ni, Y. Zhang, Y. Zhang, S. Gao, J. Liu, Z. Wang, H. He, B. Wu, X. Duan, ClC-7 deficiency impairs tooth development and eruption, Sci. Rep. 6 (2016) 19971.

[26] S. Alfaqeeh, V. Oralova, M. Foxworthy, E. Matalova, A.E. Grigoriadis, A.S. Tucker, Root and eruption defects in c-Fos mice are driven by loss of osteoclasts, J. Dent. Res. 94 (12) (2015) 1724–1731.

[27] R.A. Kesterson, L. Stanley, F. Demayo, M. Finegold, J.W. Pike, The human osteocalcin promoter directs bone-specific vitamin D-regulatable gene expression in transgenic mice, Mol. Endocrinol. 7 (3) (1993) 462–467.

[28] S. Hirota, K. Takaoka, J. Hashimoto, T. Nakase, T. Takemura, E. Morii, A. Fukuyama, K. Morihana, Y. Kitamura, S. Nomura, Expression of mRNA of murine bone-related proteins in ectopic bone induced by murine bone morphogenetic protein-4, Cell Tissue Res. 277 (1) (1994) 27–32.

[29] L.E. Zweifler, M.K. Patel, F.H. Nociti Jr., H.F. Wimer, J.L. Millan, M.J. Somerman, B.L. Foster, Counter-regulatory phosphatases TNAP and NPP1 temporally regulate tooth root cementogenesis, Int. J. Oral Sci. 7 (1) (2015) 27–41.

[30] R. Li, X. Li, M. Zhou, N. Han, Q. Zhang, Quantitative determination of matrix Gla protein (MGP) and BMP-2 during the osteogenic differentiation of human periodontal ligament cells, Arch. Oral Biol. 57 (10) (2012) 1408–1417.

[31] S.S. Hakki, D. Wang, R.T. Franceschi, M.J. Somerman, Bone sialoprotein gene transfer to periodontal ligament cells may not be sufficient to promote mineralization in vitro or in vivo, J. Periodontol. 77 (2) (2006) 167–173.

[32] A.M. Ho, M.D. Johnson, D.M. Kingsley, Role of the mouse ank gene in control of tissue calcification and arthritis, Science 289 (5477) (2000) 265–270.

[33] H. Fong, B.L. Foster, M. Sarikaya, M.J. Somerman, Structure and mechanical properties of Ank/Ank mutant mouse dental tissues–an animal model for studying periodontal regeneration, Arch. Oral Biol. 54 (6) (2009) 570–576.

[34] J. Chen, Y. Lan, J.A. Baek, Y. Gao, R. Jiang, Wnt/beta-catenin signaling plays an essential role in activation of odontogenic mesenchyme during early tooth development, Dev. Biol. 334 (1) (2009) 174–185.

[35] F. Liu, E.Y. Chu, B. Watt, Y. Zhang, N.M. Gallant, T. Andl, S.H. Yang, M.M. Lu, S. Piccolo, R. Schmidt-Ullrich, M.M. Taketo, E.E. Morrisey, R. Atit, A.A. Dlugosz, S.E. Millar, Wnt/beta-catenin signaling directs multiple stages of tooth morphogenesis, Dev. Biol. 313 (1) (2008) 210–224.

[36] T.H. Kim, C.H. Bae, E.H. Jang, C.Y. Yoon, Y. Bae, S.O. Ko, M.M. Taketo, E.S. Cho, Col1a1-cre mediated activation of beta-catenin leads to aberrant dento-alveolar complex formation, Anat. Cell Biol. 45 (3) (2012) 193–202.

[37] W.H. Lim, B. Liu, D.J. Hunter, D. Cheng, S.J. Mah, J.A. Helms, Downregulation of Wnt causes root resorption, Am. J. Orthod. Dentofac. Orthop. 146 (3) (2014) 337–345.

[38] R. Zhang, G. Yang, X. Wu, J. Xie, X. Yang, T. Li, Disruption of Wnt/beta-catenin signaling in odontoblasts and cementoblasts arrests tooth root development in postnatal mouse teeth, Int. J. Biol. Sci. 9 (3) (2013) 228–236.

[39] W.H. Lim, B. Liu, S.J. Mah, X. Yin, J.A. Helms, Alveolar bone turnover and periodontal ligament width are controlled by Wnt, J. Periodontol. 86 (2) (2015) 319–326.

[40] B. Liu, S. Chen, D. Cheng, W. Jing, J.A. Helms, Primary cilia integrate hedgehog and Wnt signaling during tooth development, J. Dent. Res. 93 (5) (2014) 475–482.

[41] H. Choi, T.H. Kim, S. Yang, J.C. Lee, H.K. You, E.S. Cho, A reciprocal interaction between beta-catenin and osterix in cementogenesis, Sci. Rep. 7 (1) (2017) 8160.

[42] C.H. Bae, J.Y. Lee, T.H. Kim, J.A. Baek, J.C. Lee, X. Yang, M.M. Taketo, R. Jiang, E.S. Cho, Excessive Wnt/beta-catenin signaling disturbs tooth-root formation, J. Periodontal Res. 48 (4) (2013) 405–410.

[43] X. Tu, Y. Rhee, K.W. Condon, N. Bivi, M.R. Allen, D. Dwyer, M. Stolina, C.H. Turner, A.G. Robling, L.I. Plotkin, T. Bellido, Sost downregulation and local Wnt signaling are required for the osteogenic response to mechanical loading, Bone 50 (1) (2012) 209–217.

[44] A.G. Robling, P.J. Niziolek, L.A. Baldridge, K.W. Condon, M.R. Allen, I. Alam, S.M. Mantila, J. Gluhak-Heinrich, T.M. Bellido, S.E. Harris, C.H. Turner, Mechanical stimulation of bone in vivo reduces osteocyte expression of Sost/sclerostin, J. Biol. Chem. 283 (9) (2008) 5866–5875.

[45] T.G. Diekwisch, The developmental biology of cementum, Int. J. Dev. Biol. 45 (5–6) (2001) 695–706.

[46] A.R. LeBlanc, R.R. Reisz, Periodontal ligament, cementum, and alveolar bone in the oldest herbivorous tetrapods, and their evolutionary significance, PLoS One 8 (9) (2013) e74697.

[47] X. Luan, C. Walker, S. Dangaria, Y. Ito, R. Druzinsky, K. Jarosius, H. Lesot, O. Rieppel, The mosasaur tooth attachment apparatus as paradigm for the evolution of the *gnathostome* periodontium, Evol. Dev. 11 (3) (2009) 247–259.